Hyperfine structure of lanthanum at sub-Doppler resolution by diode-laser-initiated resonance-ionization mass spectroscopy

R. W. Shaw, J. P. Young, D. H. Smith, A. S. Bonanno,* and J. M. Dale
Analytical Chemistry Division, Oak Ridge National Laboratory, Oak Ridge, Tennessee 37831-6142
(Received 16 August 1989)

Hyperfine structures of atomic lanthanum at sub-Doppler resolution have been recorded using diode-laser-initiated resonance-ionization and mass-spectrometric detection. Spectra were recorded for two diode-laser-pumped transitions, $^2D_{3/2}$-$^4F^\circ_{3/2}$ and $^2D_{5/2}$-$^4F^\circ_{3/2}$, at 753.9 and 819.0 nm, respectively. The linewidths observed were as narrow as 165 MHz, substantially below the expected Doppler width of 1 GHz for the 1700-K sample. Atomic hyperfine structure constants for the 13 260-cm^{-1} $^4F^\circ_{3/2}$ state were determined from the spectra: $A=-350\pm4$ MHz and $B=54\pm12$ MHz. Isotopically selective resonance ionization was achieved, even though a broadband dye laser was involved in the overall ionization process.

INTRODUCTION

Diode lasers are finding increased utility in many atomic spectroscopic techniques.[1,2] Their simplicity, narrow linewidth (to 25 MHz for off-the-shelf devices), ease of tunability, and low cost often promote their selection over competitors such as ring dye lasers. For analytical spectroscopic applications, diode lasers open broad new vistas because very high-resolution techniques can be accomplished with an inexpensive source. We have recently reported[3] the use of a 754-nm diode-laser-initiated process for 1+1+1 resonance ionization of lanthanum. In that study, the wavelength of the diode laser (first photon) was fixed and that of a tunable dye laser (second bound-bound and final bound-continuum transitions) was scanned to record two-color resonance-ionization processes in lanthanum via mass spectrometric detection, i.e., resonance-ionization mass spectrometry (RIMS). We report here the alternative experiment of fixing the dye-laser wavelength and scanning the diode laser. Sub-Doppler resolution spectra were acquired for both the $^2D_{3/2}$ and $^2D_{5/2}$ to $^4F^\circ_{3/2}$ transitions at 753.9 and 819.0 nm, respectively. Atomic hyperfine structure constants were determined for the heretofore unanalyzed 13 260-cm^{-1} $^4F^\circ_{3/2}$ state. Isotopically selective resonance ionization was also achieved for a natural abundance lanthanum sample.

The hyperfine structures of various neutral lanthanum-139 levels have been reported. The hyperfine splittings for the two levels of the ground-state term were measured by Ting[4] using a magnetic-resonance technique. Childs and co-workers[5,6] used an atomic-beam, laser-radio-frequency method to determine the atomic hyperfine constants for several levels. Both naturally occuring lanthanum isotopes possess a nonzero nuclear spin, 5 and $\frac{7}{2}$ for ^{138}La and ^{139}La, respectively. The natural abundance of the minor 138 isotope is 0.089%. Isotope-shift determinations were reported for several optical transitions by Fischer, Huhnermann, and Mandrek.[7] The lanthanum isotopes are near the neutron magic number of 82 where isotope shifts are very small; the ^{138}La-^{139}La isotope shift for several visible wavelength transitions is typically 200–400 MHz.[7]

EXPERIMENT

The experimental arrangement for these experiments was recently described.[3] A focused diode-laser beam was joined with the focused beam from a copper vapor laser-pumped rhodamine 6G dye laser in the source region of a magnetic sector mass spectrometer (see Fig. 1). Two single longitudinal mode $Ga_xAl_{1-x}As$ diode lasers were used: (a) model LT030MD0 (Sharp Corporation, Osaka, Japan), 753 nm, 3 mW and (b) model ML-3401 (Mitsubishi Electric Corp., Tokyo, Japan), 823 nm, 3 mW. The former was operated at 34.0 °C and 58 mA and the latter at −0.8 °C and 29 mA to attain the 753.9- and 819.0-nm wavelengths required for lanthanum. The operating temperature was controlled to ±0.01 °C; the rms current noise of the diode-laser power supply was specified by the manufacturer (ILX Lightwave Corp., Bozeman MT) as approximately 1 μA. A 7.5-GHz optical spectrum analyzer was used to determine the bandwidths of the diode lasers. At 819 nm the spectrum analyzer has a finesse of 100; at 754 nm the finesse is somewhat lower due to decreased reflectivity of the mirrors. The bandwidth of the 819-nm diode laser is at or below the 75-MHz full width at half-maximum (FWHM) instrumental limit of the spectrum analyzer; the apparent bandwidth of the 754-nm diode laser is ≤150-MHz FWHM, but cannot be measured to better accuracy due to the reduced analyzer finesse.

For diode laser frequency scans, a 20-mV sawtooth ramp (225-s period) from a signal generator (model 164, Wavetek Corp., San Diego CA) was impressed upon the dc bias voltage of the laser power supply to create approximately 2-mA current scans; the corresponding ranges for the frequency scans were 12 and 14.2 GHz at 754 and 819 nm, respectively. The scan ranges were determined by observing the spectrum analyzer output

 ©1990 The American Physical Society

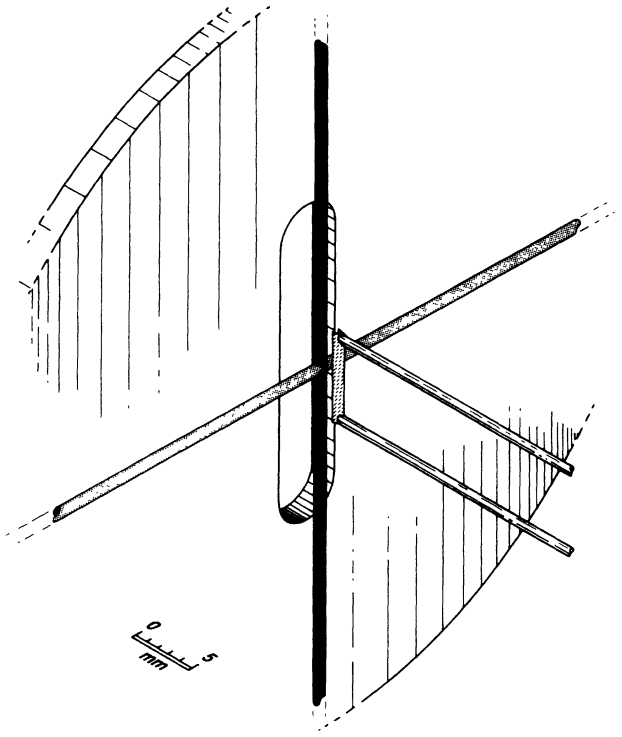

FIG. 1. Mass-spectrometer source region scaled drawing showing the diode (horizontal) and dye-laser (vertical) beams crossing between the hot filament atom source and the first plate of the mass-spectrometer ion collection lens.

with an oscilloscope as the diode-laser current was ramped; this technique resulted in approximately 1–2% precision for the frequency scan range calibrations. The frequency versus drive current was determined to be linear to better than ±0.5% by a similar technique. During the flyback portion of the sawtooth waveform, the diode-laser wavelength rapidly swept through the resonance-ionization spectrum and resulted in compressed spectra in the data that serve to mark the beginning and end of the linear portion of the voltage ramp; they appear in some of the spectral figures shown here. Note that as the drive current was increased (i.e., the diode-laser frequency was scanned to lower values), the output power also increased; power increases of approximately 15% occured for the scan ranges, and the spectra reported here have not been corrected for these power changes. The diode-laser output beam was focused to approximately a 1.2 mm diameter ($1/e^2$) at the sample location.

The dye laser was operated at 6 kHz (25-ns pulses) and produced an average power of approximately 300 mW; the spectral bandwidth was 0.3 cm^{-1}, except when the dye laser was narrowed using an intracavity etalon, in which case the bandwidth was approximately 0.05 cm^{-1}. The 584.86-nm dye-laser output beam was filtered using a 3-66 Corning glass filter (565-nm red cut-on) to eliminate amplified spontaneous emission from the output. The beam was focused to a diameter of approximately 0.8 mm by using a two-lens telescope (40/160-mm focal lengths). As shown in Fig. 1, it was joined with the diode-laser beam either as a 90° crossed beam (usual configuration) or collinearly (if noted), approximately midway between the sample filament and the first plate of the source lens of the mass spectrometer. The distance from the heated sample filament (1400 °C) to the laser beam was approximately 1 mm. Further details of the mass spectrometer were given previously.[3] The analog output from a count rate meter (0.3-s time constant) was used for recording spectra.

For isotope ratio measurements, the mass-spectrometer accelerating voltage was switched rapidly between voltages corresponding to detection of mass per charge 138, 139, and 137.5 (a background channel) at constant magnetic field while ion counts were logged. The switching protocol was controlled by a PDP/11-34 computer, and was set for dwell times of 64 ms (at mass 137.5), 576 ms (138), and 64 ms (139) and 100 counting cycles. Such mass switching methods are required to reduce effects due to time variation of atom emission from the filament.

RESULTS AND DISCUSSION

A partial energy-level diagram of neutral lanthanum is shown in Fig. 2.[8] The diode-laser-driven transitions studied here originate from the two levels of the $5d6s^2\,{}^2D_{3/2,5/2}$ ground-state term (0.0 and 1053 cm^{-1}) and terminate on the $5d6s(^3D)6p\,{}^4F^{\circ}_{3/2}$ lowest odd parity level at 13 260 cm^{-1}. From that intermediate level, the excited atoms are raised to the $^4D_{5/2}$ level at 30 354 cm^{-1} and subsequently ionized by 584.86-nm photons from the pulsed dye laser. Given the 0.3-cm^{-1} bandwidth of the dye laser, it is expected that any lanthanum atoms excited to the intermediate level at 13 260 cm^{-1} are swept on to ionization; hence scans of the diode-laser frequencies should yield hyperfine structures for the 0–13260 and 1053–13 260 cm^{-1} transitions.

A scan of the 0–13260 cm^{-1} transition of ^{139}La is presented in Fig. 3. The features at the two extremes of the spectrum are compressed spectra as noted in the experimental section; the actual spectrum extends from −1.0 to 6.0 GHz. The strongest line in Fig. 3 (shown arbitrarily as 0.0 GHz) corresponds to a count rate of 700 counts per second (cps); its linewidth is 165 MHz FWHM. The spectrum was recorded using a diode-laser power of 0.1 mW created by attenuating the full beam power with a neutral density filter.

A second spectrum was taken with the dye laser tuned to 586.54 nm instead of 584.86 nm. For this latter case the ionization mechanism is similar to that shown in Fig. 2, except that the final bound atomic level is the $^2F_{5/2}$ level at 30 305.6 cm^{-1}.[3] The spectrum was identical to that shown in Fig. 3. Thus the sharp features of the spectrum are independent of the second intermediate level involved in the excitation process. The spectrum was also reproduced when the 584.86-nm copper vapor laser-pumped dye laser was replaced with a 1-μs pulsed, flashlamp-pumped rhodamine 6G dye laser (at the same wavelength) with a spectral bandwidth of 3 cm^{-1}. The spectral structure is thus representative of the 0–13 260 cm^{-1} transition and is not due to laser-dependent parameters such as cavity mode structure or pulse length. At

higher diode-laser powers than those used for Fig. 3, the spectral resolution degraded. As reported earlier,[3] the ion current begins to saturate at laser powers of approximately 2 mW. In addition to power broadening, some of the resolution loss is due to the growth of a secondary spectrum as shown in Fig. 4. Spectra are presented for diode-laser powers of 0.2, 0.5, and 2.6 mW; the relative count rate scale factors are 6.7, 3.3, and 1.0, respectively. As the power is increased, a duplicate spectrum arises at slightly lower frequency than the main spectrum. This secondary spectrum will be discussed further below.

The sharp structure seen in Fig 3 is due to the atomic hyperfine structure of the $^2D_{3/2}$ and $^4F^\circ_{3/2}$ levels. Ting has reported[4] the splittings for the $^2D_{3/2}$ ground term; they are shown in the left-hand energy-level diagram of Fig. 5. The intervals of the $^4F^\circ_{3/2}$ upper level are unknown. The ^{139}La nuclear spin of $\frac{7}{2}$ results in fourfold

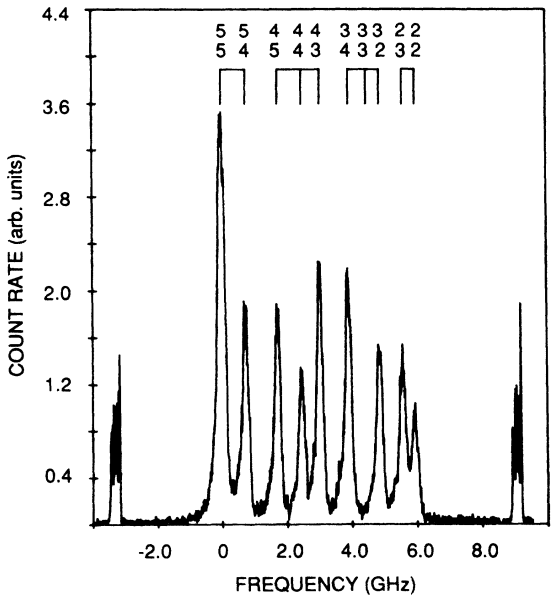

FIG. 3. 0–13 260 cm^{-1} hyperfine structure of ^{139}La at 754 nm. See the text for an explanantion of the artifacts at the extremes of the scan.

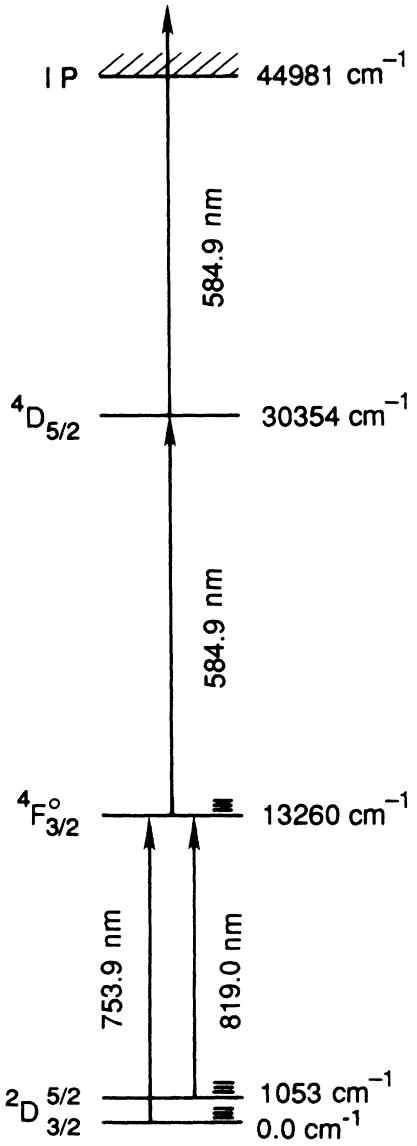

FIG. 2. Partial energy-level diagram of neutral lanthanum.

splitting for $J=\frac{3}{2}$ levels, with the hyperfine quantum number F ranging from 2 to 5.[9] The $\Delta F=0, \pm 1$ selection rule predicts ten allowed hyperfine lines, one more than is apparent in the spectrum shown in Fig. 3. A computer program was written that performed two tasks. It first identified the F quantum numbers associated with each line in the spectrum. Second, it found values for the magnetic dipole and electric quadrupole constants (A and B, respectively) for the 13 260-cm^{-1} level via a least-squares fitting routine that produced a calculated spectrum that most closely matched that observed. The de-

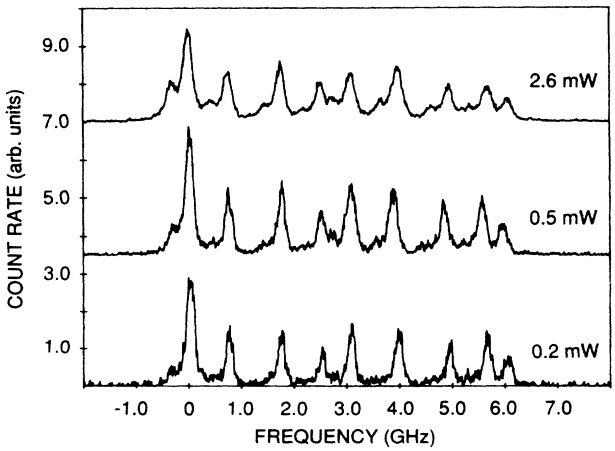

FIG. 4. Diode-laser power dependence of the ^{139}La 0–13 260 cm^{-1} hyperfine spectrum. Spectra (offset for clarity) are shown for diode-laser powers of 0.2, 0.5, and 2.6 mW; the relative count rate scale factors are 6.7, 3.3, and 1.0, respectively.

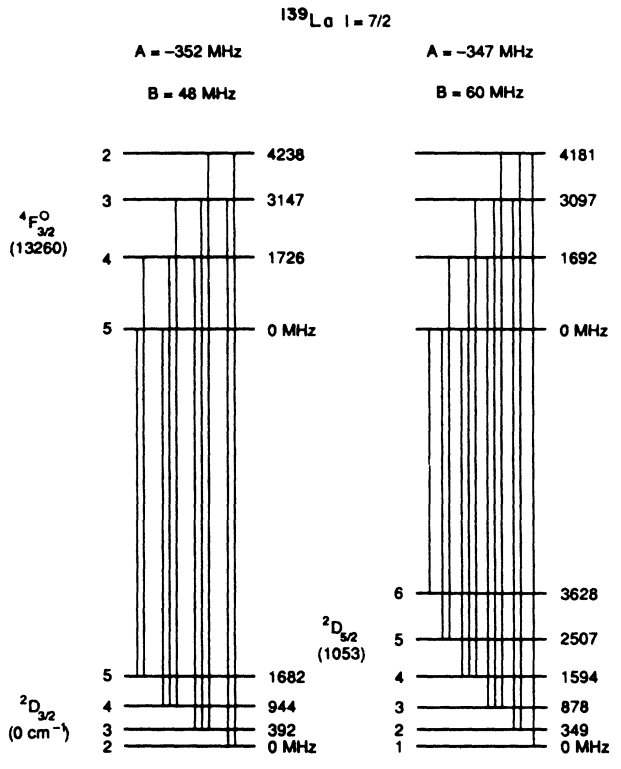

FIG. 5. Partial energy-level diagram for ^{139}La, showing atomic hyperfine splittings. The splittings of the $^2D_{3/2}$ and $^2D_{5/2}$ levels are due to Ting (Ref. 4).

tails of the program are available from the authors. The resulting upper level intervals are shown in Fig. 5. The A and B constants, with corresponding standard deviation of the mean, derived for the ^{139}La 13 260-cm^{-1} level are

$$A = -352 \pm 6 \text{ MHz} ,$$

$$B = 48 \pm 15 \text{ MHz} .$$

The largest deviation for any of the nine observed lines from the corresponding calculated position is 20 MHz. For some spectra, fine adjustment of our frequency scale calibration was made using the splittings of pairs of lines separated only by one of Ting's ground-state level splittings, which are known to much greater accuracy and precision than is possible here. That correction corresponded to 1% changes in our scale. The calculated spectrum is shown at the top of Fig. 3 as a stick spectrum. The F quantum numbers of the upper and lower levels are shown as the upper and lower numbers, respectively.

The $F=3$ to $F'=3$ line is missing from the resonance ionization spectrum. Line intensity calculations made by using $6J$ symbols[10] were performed for the lines of the spectrum. The calculated intensity of the $F=3$ to $F'=3$ line is identically zero. The calculated relative intensities of the other lines (see Table I) match those observed experimentally to within ±15%. This result indicates that substantial intensity alterations due to optical pumping effects noted by other workers[11] are absent for these measurements.

Why is the resolution of the spectrum shown in Fig. 3 so high? The sample filament was operated at 1700 K, and for a particle mass of 139 amu, the free gas Doppler width (in MHz) should be

$$\Delta\nu = (7.16\times10^{-7})\nu(T/M)^{1/2} = 995 ,$$

where $\Delta\nu$ is the Doppler-broadened linewidth (FWHM), ν is the frequency of the transition, T is the temperature (K), and M is the particle mass. The spectral width exhibited in Fig. 3 is approximately one-sixth the calculated Doppler width. The geometric factor derived from crossing 1-mm-diam beams 1 mm from a point source of atoms reduces the predicted Doppler width, but not nearly enough to explain the observed spectrum. Some process that effects additional atom-beam collimation must be operative; the most likely candidate is collection of photoions from a restricted spatial region. An atom-beam collimation ratio of approximately 10:1 would be required to yield Doppler widths of a few hundred megahertz.

The sample filament is probably more like a line source of atoms after its first heating due to migration of lanthanum over the length of the filament (approximately 0.5 cm); such behavior on metal surfaces has been observed for uranium.[12] Atom trajectories originating from points off the midpoint of the filament and passing through the crossed-beams intersection would be normal to the diode-laser beam and would not contribute to Doppler broadening.

The mass spectrometer is, of course, a focusing instrument and collects ions from a specific focal volume in space. In the experiment that yielded Fig. 3, the posi-

TABLE I. Calculated relative hyperfine structure component intensities for ^{139}La at 753.9 and 819.0 nm.

753.9 nm ($^2D_{3/2}$-$^4F°_{3/2}$)		819.0 nm ($^2D_{5/2}$-$^4F°_{3/2}$)	
Component[a]	Calculated relative intensity[b]	Component[a]	Calculated relative intensity[b]
		5/6	2.17
5/5	1.98	5/5	0.51
5/4	0.77	5/4	0.07
4/5	0.77	4/5	1.83
4/4	0.48	4/4	0.74
4/3	1.0	4/3	0.19
3/4	1.0	3/4	0.69
3/3	0.0	3/3	0.73
3/2	0.75	3/2	0.33
2/3	0.75	2/3	0.25
2/2	0.50	2/2	0.50
		2/1	0.50

[a]Upper level F/lower level F; the components are listed in order of ascending frequency.

[b]Calculated using 6-j symbols (Ref. 10)

tions of the crossing diode and dye-laser beams were adjusted for maximum ion current through the mass spectrometer, and their crossing point is thus near the focal point of the ion lens. In this particular case, the dye-laser beam was parallel to the length of the sample filament and the mass-spectrometer slit; the diode-laser beam was perpendicular to the filament. The foci of both beams are projected at great distances (>1 m), so the intersection-volume is approximately that of two crossed cylinders.

The focal volume from which the mass spectrometer collects ions is not precisely known. An estimate of that volume was made by translating the line of the diode-laser beam along the propagation axis of the dye-laser beam while maintaining right angle crossing; the extent of laser beam overlap should be relatively unaffected by this motion. The motion is experimentally simple due to the compact nature of the diode-laser source. Translating the diode-laser beam 0.64 mm from the position corresponding to the maximum two-color count rate reduced the count rate to 20% of the maximum value. The ion beam intensity is thus very sensitive to submillimeter motions of the laser beam crossing point.

Another method employed to gauge the active volume of the combined laser beam crossing–mass-spectrometer focus was to examine the spectral resolution for alternative laser beam geometries. Three geometries were examined: (a) the geometry described above and shown in Fig. 1; (b) collinear laser beams with the propagation direction parallel to the filament (and mass-spectrometer slit); and (c) collinear beams, but with the propagation direction perpendicular to the filament. The linewidth of the strong $F=5$ to $F'=5$ line was 260 MHz FWHM for geometry (b). The spectral resolution of each case was similar to the others, i.e., widths much less than 995 MHz. For collinear beams, the laser beam intersection volume is substantially greater, and the lasers interact with a larger set of atomic angular trajectories. The Doppler-limited spectral width would be correspondingly greater, unless the ion optics are unable to collect the photoions from off-axis regions.

The secondary spectrum seen in Fig. 4 and noted above could possibly be due to ionization of atoms at a secondary spatial position along the perpendicular diode-laser beam. A stray dye-laser beam (e.g, a back reflection from the vacuum chamber exit window) intersecting the diode-laser beam at a second point would excite and ionize atoms with a different trajectory from the filament. The approximately 200-MHz shift between the two spectra indicates a 17° angular difference between the trajectories of the atoms, assuming a point source. At a distance of 1 mm from the filament, the 17° angular difference corresponds to a separation of 0.3 mm. The intensity of the secondary spectrum is weak at low diode-laser power, but as the primary spectrum saturates, the weak spectrum attains comparable apparent intensity. Alternatively, either of the laser beam foci or the ion collection focus could exhibit an aberration-derived double image and hence two active volumes for ion creation or collection.

When an intracavity etalon was inserted into the dye-laser oscillator to narrow its spectral output, the spectrum shown in Fig. 6 was recorded. The diode laser power for this scan was approximately 2 mW. The dye-laser spectral bandwidth is now approximately 0.05 cm^{-1} (i.e., 1500 MHz); the presence of the dye-laser frequency required to complement all hyperfine components of the first transition can no longer be assumed. A partial spectrum is observed. The specific partial spectrum recorded was dictated by the fact that the dye-laser etalon tilt was adjusted for maximum ion count rate while the diode-laser frequency was fixed at the $F=5$ to $F'=5$ hyperfine component of the 13 260-cm^{-1} transition.

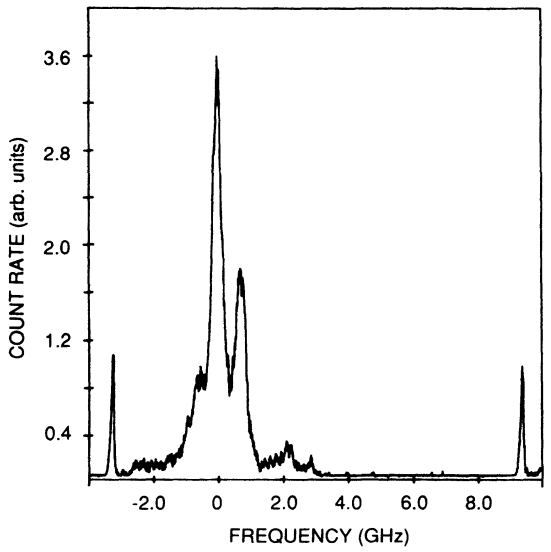

FIG. 6. 0–13 260 cm^{-1} hyperfine structure of ^{139}La as shown in Fig. 3, except with a line narrowing etalon inserted in the dye-laser oscillator.

The $^2D_{5/2}$ ground-state-term level of ^{139}La at 1053 cm^{-1} is also populated for the atoms that evolve from the

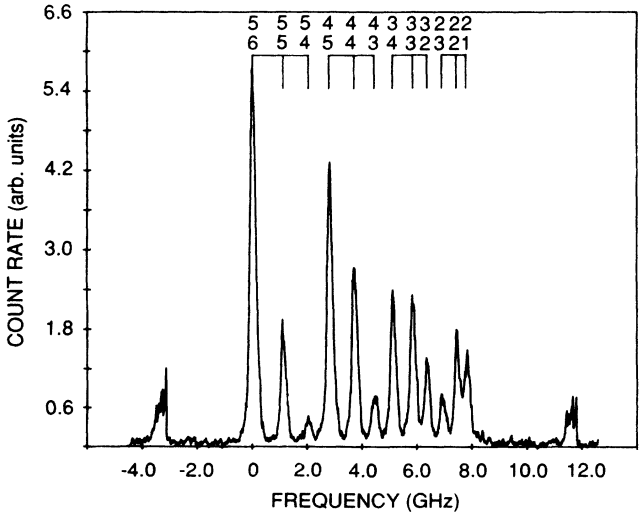

FIG. 7. 1053–13 260 cm^{-1} hyperfine structure of ^{139}La at 819 nm.

heated filament. A high-resolution spectrum of the 1053–13 260 cm^{-1} transition was recorded with the aid of an 819-nm diode-laser (see Fig. 7). A crossed-beam geometry was employed, and the dye-laser wavelength was 584.86 nm as in Fig. 3. No intracavity etalon was used. The overall excitation and ionization scheme is identical to that described previously except for the changed first step. Comparable spectral resolution was observed. The linewidth of the lowest energy hyperfine component is 245 MHz (FWHM). The spectrum comprises 12 lines, and the F quantum number assignments are shown in the figure.

The ion count rate for the $F=6$ to $F'=5$ component was measured at diode-laser powers between 0.3 and 5.4 mW; no deviation from linearity was detected. The ion yield corresponding to this transition is substantially lower than that for the $F=5$ to $F'=5$ component of the 0–13 260 cm^{-1} transition. For diode-laser powers of approximately 2 mW and a filament temperature of 1350 °C, the relative ion yield is 45:1 for the optical process beginning from the ground state relative to that from the 1053-cm^{-1} level (i.e., 754 versus 819-nm excitation). Correcting for the J-degeneracy difference, the ratio becomes 68:1. At a higher filament temperature (1500 °C), the latter ratio drops to 38:1, consistent with a higher population of the 1053-cm^{-1} level at the higher temperature. Such large ratios are incongruent with a naive Boltzmann population distribution picture if similar oscillator strengths are assumed for the $^2D_{3/2}$ and $^2D_{5/2}$ to $^4F^{\circ}_{3/2}$ transitions. Those relative oscillator strengths are unknown to us; however, Meggers's compilation of spectral-line emission intensities[13] suggests that the 754-nm La I line is substantially stronger than the one at 819 nm. The former is listed with an intensity of 85, while the latter is absent from the table. A nearby line at 820 nm with an intensity of 7 is shown, indicating adequate sensitivity in this spectral region to have observed the 819-nm line at approximately tenfold lower intensity. If the relative oscillator strengths were known accurately, it would be possible to measure the relative populations of these initial atomic states evolved from the heated filament by this technique. Such a measurement is of practical importance for gauging the ultimate sensitivity of RIMS because all atoms in initial states not addressed by wavelengths utilized in an ionization scheme are lost to the measurement.

The hyperfine structure of the $^4F^{\circ}_{3/2}$ level derived above can be confirmed using the 1053–13 260 cm^{-1} transition spectral information of Fig. 7. The hyperfine structure of the 1053-cm^{-1} level is known from Ting's work[4] (see Fig. 5). The A and B coefficients, with corresponding standard deviation of the mean, for the 13 260-cm^{-1} level as calculated from the spectrum shown in Fig. 7 are

$$A = -347 \pm 2 \text{ MHz}$$

$$B = 60 \pm 8 \text{ MHz} .$$

These results are in good agreement with those derived above from the 0–13 260 cm^{-1} hyperfine structure. The relative line intensities agree to within ±15% with the calculated values (see Table I).

The efficiency of the ionization process initiated with the 0–13 260 cm^{-1} transition is sufficiently high that the corresponding spectrum could be recorded for the minor 138 isotope in a natural abundance lanthanum sample. This was accomplished by changing the accelerating voltage at constant magnetic field to bring the minor isotope into focus at the exit slit of the mass spectrometer. The 0–13260 cm^{-1} hyperfine structures for ^{138}La and ^{139}La are shown as the upper and lower traces of Fig. 8. To record the ^{138}La spectrum, it was necessary to raise the filament temperature to 1480 °C (from 1300 °C for ^{139}La) and increase the count rate meter sensitivity by fivefold. The maxima of the strongest component lines for the two individual spectra represent 120 and 800 cps for ^{138}La and ^{139}La, respectively; the diode-laser power was 0.4 mW. The weak character of the 1053–13 260 cm^{-1} transition prevented observation of that spectrum for ^{138}La at natural abundance.

As can be seen in Fig. 8, the ^{138}La spectrum extends both to higher and lower frequencies than that for ^{139}La. The spectral offset of the lowest frequency lines was used to attempt isotopically selective ionization. Ion counts were conducted for ^{138}La and ^{139}La at each of the two maximum response frequencies (−670 and 0.0 MHz). This frequency separation corresponds to a diode-laser drive current difference of 0.12 mA. The results are summarized in Table II.

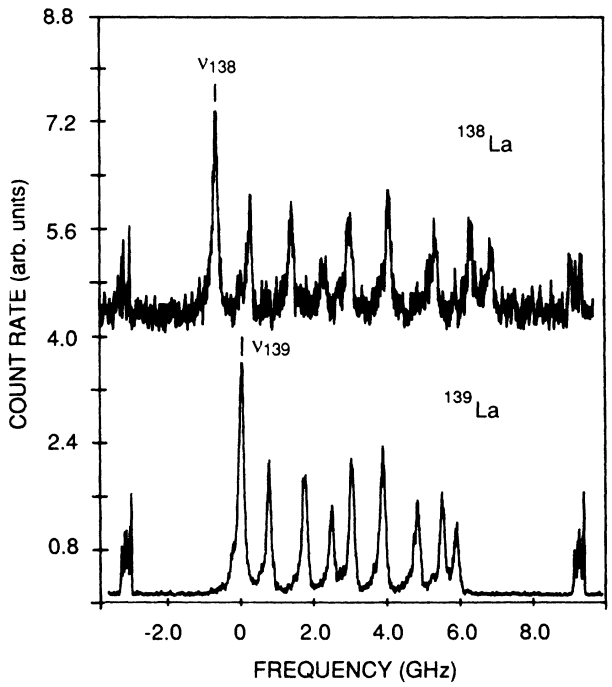

FIG. 8. 0–13 260 cm^{-1} hyperfine structure for ^{138}La (upper trace, offset vertically for clarity) and ^{139}La (lower trace) for a natural abundance sample. For the ^{138}La trace, the filament temperature was raised from 1300 to 1480 °C and the count rate meter sensitivity was raised fivefold. The labeled lines were utilized for isotopically selective ionization.

TABLE II. ^{139}La-to-^{138}La apparent isotope ratios for two-color, diode-laser-initiated RIMS and thermal-ionization mass spectrometry for a natural abundance sample.

Diode laser frequency selected for isotope	Raw ion counts for mass[a,b] 138	139	Apparent 139/138 isotope ratio (± standard deviation)	Selectivity factor based upon the apparent ratio
^{138}La	198	715	31.3±6	30
^{139}La	20	50 459	22 700±6000	25
None[c]	312	32 025	925±65[d]	(1.00)

[a]Uncorrected for the 9:1 dwell time ratio favoring mass 138.
[b]Sum of seven ion count measurements on one sample for the ^{138}La laser frequency, nine for the ^{139}La laser frequency, and three for thermal ionization.
[c]Thermal ionization measurement.
[d]Accepted value 1123.

These preliminary ion counting results indicate that the apparent ^{139}La to ^{138}La isotope ratio of a natural abundance lanthanum sample can be changed from about 30 to over 22 000 by judicious selection of diode-laser excitation frequency, a change of over 700-fold. The selectivity factor for ^{138}La resonance ionization over ^{139}La is 30; the inverse selectivity factor is 25. These results are in good agreement with selectivities predicted using the signal strength at the indicated hyperfine component of each isotope (see Fig. 8) along with the corresponding background at that frequency due to the other isotope. The value reported for the thermally produced ions differs from the International Union of Pure and Applied Chemistry recommended value (925±65 versus 1123).[14] This is probably due to poor counting statistics, but isotopic fractionation may also have had an effect; the sample had been in use for considerable time when this measurement was made. The natural variation of isotopic abundance for lanthanum is apparently unknown.[14]

The selectivity factors are only approximate due to the poor counting statistics resulting from the few ^{138}La counts collected, especially for the case where the diode-laser frequency was set for selection of ^{139}La. More accurate results must await a sample that is enriched in ^{138}La and better frequency control of the diode laser. Narrow bandwidth laser-derived isotopic selectivity can be used to reduce the dynamic range required of a mass spectrometer for isotope ratio measurements of elements with widely different isotopic abundances; the selectivity due to the diode laser can serve to skew the apparent abundances toward equality. Recall that the isotopic selectivity achieved here was accomplished with a simple and inexpensive diode laser. The isotopic selectivity of the mass spectrometer can be utilized for the spectroscopy of rare isotopes in the presence of more abundant isotopes of the same element.[15]

CONCLUSIONS

High-resolution 1+1+1 resonance ionization spectra were acquired for the 0.0–13 260 cm^{-1} and 1053–13 260 cm^{-1} transitions of lanthanum-139 by current tuning a diode laser. The hyperfine structure of the 13 260-cm^{-1} level was derived from the spectra. The spectral linewidths were as narrow as 165 MHz. This sub-Doppler resolution is thought to be due to the minute effective volume for photoion extraction. The geometry of the laser beams—perpendicular or collinear—had little effect on the observed spectral resolution. The resolution is not as yet limited by the linewidth of the scanning diode laser; further improvements in resolution (and isotopically selective ionization) may be possible by changes in the ion optics of the mass spectrometer.

Partial isotopic selectivity was achieved for ^{138}La and ^{139}La. The apparent isotope ratio for a natural abundance sample could be altered more than 700-fold by careful selection of diode-laser wavelengths. Studies are currently underway using a sample enriched in ^{138}La to make more precise measurements of the ^{138}La 13 260-cm^{-1} level hyperfine structure, the ^{138}La-to-^{139}La isotope shifts for the 754- and 819-nm transitions, and the optimized selectivity factors for isotopically selective resonance ionization by this 1+1+1 process.

ACKNOWLEDGMENTS

Research sponsored by the Office of Energy Research, U. S. Department of Energy, under Contract No. DE-AC05-84OR21400, with Martin Marietta Energy Systems, Inc. The authors thank J. M. Ramsey, W. B. Whitten, and P. R. Blazewicz for helpful discussions. One of us (A.S.B.) acknowledges support from the Oak Ridge Associated Universities.

*Present address: Department of Chemistry, University of Idaho, Moscow, ID 83843.

[1]J. Lawrenz and K. Niemax, Spectrochim. Acta **44B**, 155 (1989).
[2]J. R. Brandenberger, Phys. Rev. A **39**, 64 (1989).
[3]R. W. Shaw, J. P. Young, and D. H. Smith, Anal. Chem. **61**, 695 (1989)
[4]Y. Ting, Phys. Rev. **108**, 295 (1957).

[5]W. J. Childs and L. S. Goodman, Phys. Rev. A **20**, 1922 (1979).
[6]W. J. Childs and U. Nielsen, Phys. Rev. A **37**, 6 (1988).
[7]W. Fischer, H. Huhnermann, and K. Mandrek, Z. Phys. **269**, 245 (1974).
[8]W. C. Martin, R. Zalubas, and L. Hagan, *Atomic Energy Levels-The Rare Earth Elements,* Natl. Stand. Ref. Data Ser., Natl. Bur. Stand. (U.S.), NBS-60 (U.S. GPO, Washington, D.C., 1978).
[9]W. J. Childs, Case Stud. At. Phys. **3**, 215 (1973).
[10]A. R. Edmonds, *Angular Momentum in Quantum Mechanics* (Princeton University Press, Princeton, 1957).
[11]B. A. Bushaw, B. D. Cannon, G. K. Gerke, and T. J. Whitaker, Opt. Lett. **11**, 422 (1986).
[12]D. H. Smith, W. H. Christie, and R. E. Eby, Int. J. Mass Spectrom. Ion Phys. **36**, 301 (1980).
[13]W. F. Meggers, C. H. Corliss, and B. F. Scribner, *Tables of Spectral-line Intensities, Part I, Arranged by Elements,* 2nd ed., Natl. Bur. Stand. (U.S.) Monograph 145 (U.S. GPO, Washington, D.C. 1975), p. 133.
[14]N. E. Holden *et al.*, Pure Appl. Chem. **52**, 2349 (1980).
[15]C. A. Miller, R. Engleman, Jr., and R. A. Keller, J. Opt. Soc. Am. B **2**, 1503 (1985).

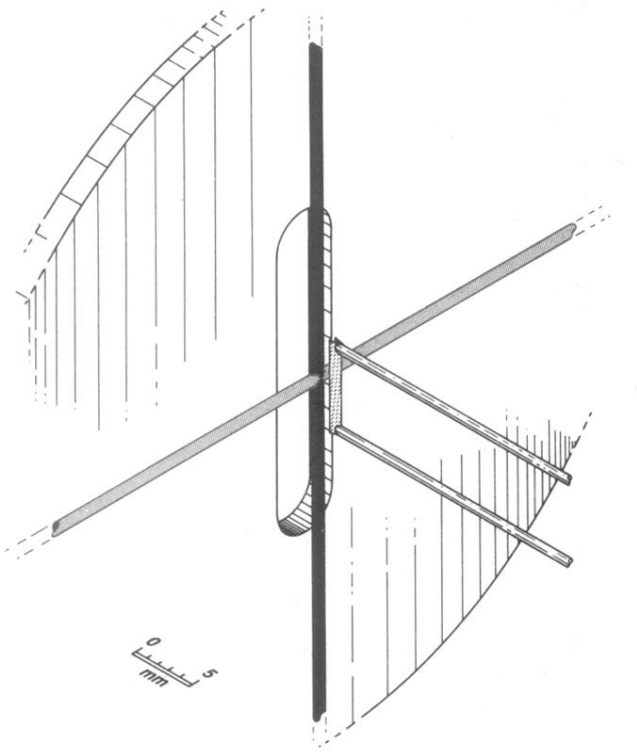

FIG. 1. Mass-spectrometer source region scaled drawing showing the diode (horizontal) and dye-laser (vertical) beams crossing between the hot filament atom source and the first plate of the mass-spectrometer ion collection lens.